

1 **Ozone and Aerosol Optical Depth Retrievals Using the Ultraviolet Multi-Filter Rotating**
2 **Shadow-band Radiometer**

3
4 Joseph Michalsky¹ and Glen McConville^{1,2}

5
6 ¹Global Monitoring Laboratory, National Oceanic and Atmospheric Administration,
7 325 Broadway, Boulder, Colorado 80305 USA

8 ²Cooperative Institute for Research in Environmental Sciences, University of Colorado,
9 216 UCB, Boulder, Colorado 80309 USA

10
11 *Correspondence to:* Joseph Michalsky (joseph.michalsky@noaa.gov)

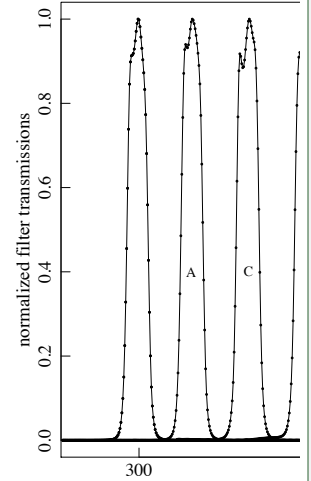
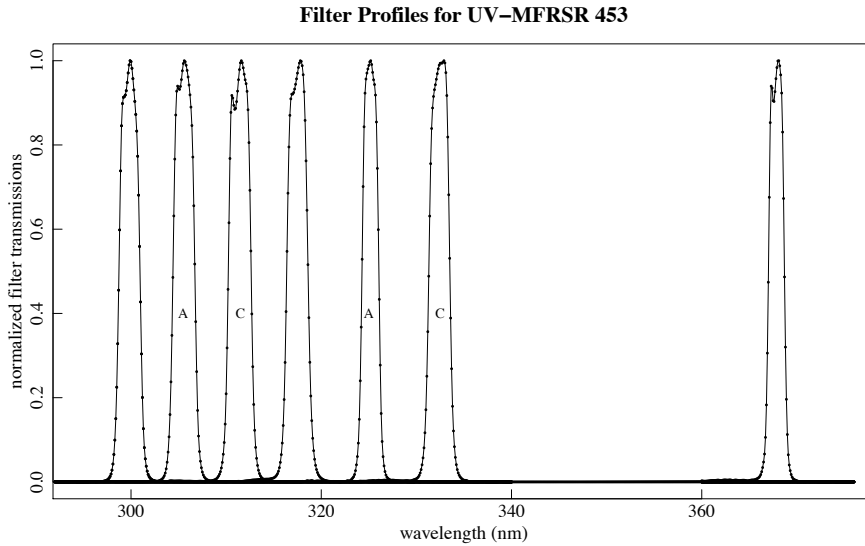
12
13
14 **Abstract:** The ultraviolet multi-filter rotating shadowband radiometer (UV-MFRSR) is a seven-
15 channel radiometer with narrowband filters centered between wavelengths 300 and 368 nm. Four
16 of the middle wavelengths in this device are near those used in the Dobson spectrometer to
17 retrieve ozone column abundance. In this paper measurements from Mauna Loa Observatory
18 (MLO) were used, first, to calibrate the instrument using the Langley plot method, and,
19 subsequently, to derive column ozone and aerosol optical depths. The ozone derived from the
20 UV-MFRSR was compared to the ozone measured by a Dobson spectrophotometer that operates
21 daily at the MLO resulting in column values within about 1 DU on average for 43 days in 2018.
22 The aerosol optical depth (AOD) retrievals are more challenging. Generally, the AOD increases
23 with wavelength between 305 and 332 nm; not what is expected given the typical AOD
24 wavelength dependence at visible wavelengths. An example of this behavior is discussed, and
25 research by others is cited that indicates similar behavior at these wavelengths, at least for the
26 low aerosol optical depth conditions encountered at high altitude sites.

27
28
29 **Ozone Retrieval Introduction**

30
31 Most historical network measurements of column ozone from the surface used Dobson or
32 Brewer spectrometers, and these continue as the predominant ozone measurement instruments
33 today. Brief explanations of these two devices and comparisons of concurrent and collocated
34 measurements of total column ozone are given in Staehelin et al. (2003). Gao et al. (2001)
35 demonstrated that ozone could be retrieved using the ultraviolet multi-filter rotating shadow-
36 band radiometer (UV-MFRSR), which agreed with those values retrieved from either collocated
37 Dobson and/or Brewer spectrophotometers to within 1-2%.

38
39 The wavelengths used for ozone retrievals in the UV-MFRSR more closely match wavelengths
40 in the Dobson rather than the Brewer spectrophotometer. Typically, ozone retrieved from the
41 Dobson uses the AD wavelength pairs 'A' 305.5/325.4 and 'D' 317.6/339.8. Since there is no
42 filter near 339.8 nm, the UV-MFRSR uses filters near the 'A' pair and the Dobson 'C' pair
43 311.5/332.4. The filters in the UV-MFRSR that are used for ozone measurements are nominally
44 the 305/325 nm pair and the 311/332 nm pair with carefully measured profiles of these filters
45 used for actual retrievals. [Normalized filter profiles for UV-MFRSR 453 are shown in Figure 1.](#)

Deleted: Normalized filter profiles for UV-MFRSR 453 are shown in Figure 1.



48 Figure 1. Normalized filter profiles of UV-MFRSR 453 used in this study. The wavelength-dependent ozone
 49 absorption function and Rayleigh scattering function were convolved with these profiles to produce effective
 50 absorption and scattering corrections. 'A' and 'C' pairs used for ozone retrievals are noted. Central
 51 wavelength/full width at half maximum (nm): 299.9/2.2, 305.6/2.3, 311.4/2.4, 317.5/2.3, 325.1/1.8, 332.4/2.2,
 52 367.8/1.7.

53
 54 The basic procedure for ozone retrievals consists of measuring extinction at two wavelengths
 55 with one chosen to be more strongly attenuated than the other in the Hartley-Huggins ultraviolet
 56 bands. The basic extinction equation can be written

$$I(\lambda) = I_0(\lambda) \cdot \exp [-\tau_{ray}(\lambda)m_{ray}(\lambda) \left(\frac{P}{P_0}\right) - \tau_{oz}(\lambda)m_{oz}(\lambda) - \tau_{aer}(\lambda)m_{aer}(\lambda)] \quad (1)$$

57
 58 or, equivalently,

$$V(\lambda) = V_0(\lambda) \cdot \exp [-\tau_{ray}(\lambda)m_{ray}(\lambda) \left(\frac{P}{P_0}\right) - \tau_{oz}(\lambda)m_{oz}(\lambda) - \tau_{aer}(\lambda)m_{aer}(\lambda)] \quad (2)$$

59
 60 since the ratios I/I_0 and V/V_0 are equal.

61
 62 In these equations:

- 63 $I(\lambda)$ = spectral irradiance measured by the instrument at the surface
- 64 $I_0(\lambda)$ = spectral irradiance measured by the instrument at the top of the atmosphere
- 65 $V(\lambda)$ = signal (voltage) measured by the instrument at the surface

Moved down [1]:
 Figure 1. Normalized filter profiles of UV-MFRSR 453 used in this study. The wavelength-dependent ozone absorption function and Rayleigh scattering function were convolved with these profiles to produce effective absorption and scattering corrections. 'A' and 'C' pairs used for ozone retrievals are noted. Central wavelength/full width at half maximum (nm): 299.9/2.2, 305.6/2.3, 311.4/2.4, 317.5/2.3, 325.1/1.8, 332.4/2.2, 367.8/1.7.

Moved (insertion) [1]

Deleted: for ozone retrievals

$V_0(\lambda)$ = signal (voltage) measured by the instrument at the top of the atmosphere
 τ 's = optical depths for Rayleigh scattering (ray), ozone (oz), and aerosol (aer)
 P, P_0 = atmospheric pressure at the measurement site and at sea level, respectively
 m 's = air masses for Rayleigh, ozone, and aerosol relative to a vertical path; they differ slightly because each has a different distribution with altitude in the atmosphere. [The Rayleigh and ozone air masses were calculated using Bodhaine et al., \(1999\) and Komhyr and Evans \(2008\), respectively.](#)

Deleted: The Rayleigh and ozone air masses were calculated using Bodhaine et al., (1999) and Komhyr and Evans (2008), respectively.

76 If we write ozone optical depth as $\tau_{oz} = \alpha_{oz} \cdot \eta_{oz}$, where α_{oz} is the ozone absorption coefficient
 77 and η_{oz} is the abundance of ozone, we can solve for η_{oz} by rearranging terms in two versions of
 78 eqn. (2) representing the two wavelengths in the pair (the longer wavelength is indicated by
 79 primes). Therefore, dropping the explicit λ dependence for clarity, we get for ozone abundance
 80

$$\eta_{oz} = \frac{N - (\tau_{ray} - \tau'_{ray})m_{ray}(P/P_0) - (\tau_{aer} - \tau'_{aer})m_{aer}}{(\alpha_{oz} - \alpha'_{oz})m_{oz}}, \quad (3)$$

81
 82 where N is defined as
 83

$$N = \ln(V_0/V'_0) - \ln(V/V').$$

84
 85 Since all of the parameters of eqn. (3) are known or can be calculated, one could solve for η_{oz} if
 86 the term $(\tau_{aer} - \tau'_{aer})$, i.e., the aerosol optical depths at the two wavelengths were known. To
 87 curtail this requirement, the 'A' and 'C' wavelength pairs are used, and the assumption is made
 88 that since the wavelength separation of each pair is nearly the same and the wavelength
 89 dependence over this small wavelength region is expected to be nearly linear, subtraction of eqn.
 90 (3) applied to each pair will come very close to eliminating the aerosol terms because subtraction
 91 of aerosol terms should be near zero if these assumptions hold. The resulting equation used to
 92 calculate ozone is
 93
 94

$$\eta_{oz} = \frac{N_1 - N_2 - [(\tau_{ray} - \tau'_{ray})_1 - (\tau_{ray} - \tau'_{ray})_2]m_{ray}(P/P_0)}{[(\alpha_{oz} - \alpha'_{oz})_1 - (\alpha_{oz} - \alpha'_{oz})_2]m_{oz}}, \quad (4)$$

95
 96 where
 97

$$N_1 = \ln(V_{o,305}/V'_{o,325}) - \ln(V_{305}/V'_{325}),$$

98
 99 and
 100

$$N_2 = \ln(V_{o,311}/V'_{o,332}) - \ln(V_{311}/V'_{332}).$$

103

108
109
110
111
112
113
114
115
116
117
118
119
120
121
122
123
124
125
126
127
128
129
130
131
132
133
134
135
136
137
138
139
140

Calibration and Ozone Measurement Comparisons

The Langley calibration of the UV-MFRSR was performed at NOAA's Mauna Loa Observatory (Latitude = 19.5362°N; Longitude = 155.5763°W; 3397 m). The height of the observatory often allows measurements to be made in clean, free-tropospheric air above the marine boundary layer, especially in the morning hours.

UV-MFRSR data were obtained on 242 days in 2018 beginning on 14 February and ending on 15 October. There were 139 successful Langleys during this period that produced estimated Vo's with only 27 of these during the afternoon hours. Looking at the retrieved Vo's as a function of time there is a hint of a decrease, but not one filter indicates a statistically significant decline, therefore, averages of Vo's over the entire period are used in the ozone and aerosol retrievals.

The process used to choose acceptable Langleys (Michalsky et al., 2001) eliminates Langleys that are influenced by large changes in ozone during a Langley plot. Further, rarely did the standard deviation of the ozone sampled change by more than 5 DU during a morning or afternoon when Langleys plots are sampled. This small change is typical for this low latitude.

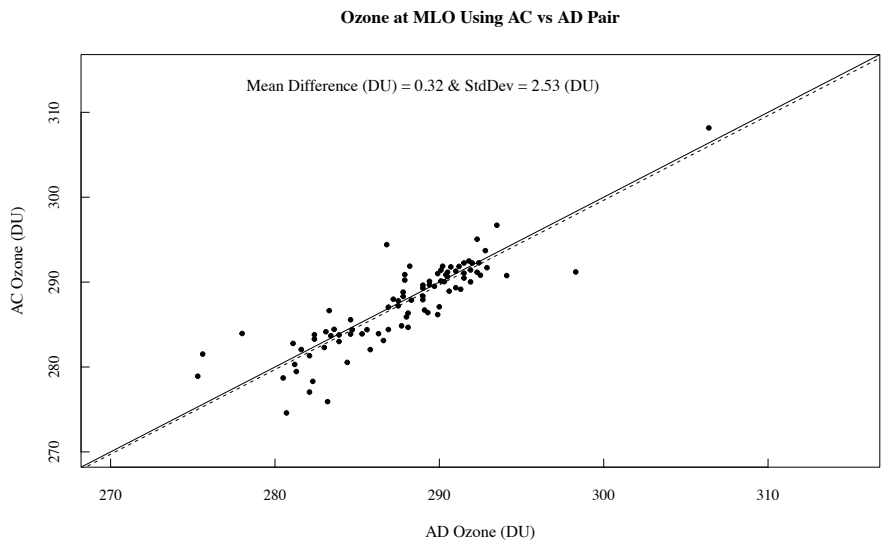
Ozone is a standard measurement at NOAA's Mauna Loa Observatory and has been made with near continuous sampling since 1963. The Dobson spectrophotometer there makes AD paired measurements to determine ozone using absorption coefficients measured by Bass and Paur (1985). No estimate of the ozone column below the observatory, which could be on the order of 5% of the column total at sea level, is made. Therefore, the column measurements made using the UV-MFRSR can be directly compared to the Dobson column measurements if one uses the Bass and Paur (1985) absorption cross-sections for the UV-MFRSR channels.

Since the Dobson generally uses the AD pair for the total column ozone calculation, we investigated the difference between AC and AD Dobson retrievals on two clear days at Mauna Loa that were used for Langley calibrations of the Dobson thus giving us more than the operational 1000, 1200, and 1400 local time ozone measurements. It is important to assess any differences since the UV-MFRSR uses wavelengths close to the AC pair for its ozone retrievals. Figure 2 illustrates the difference between Dobson measurements with the two different

Moved down [2]: The process used to choose acceptable Langleys (Michalsky et al., 2001) eliminates Langleys that are influenced by large changes in ozone during a Langley plot. Further, rarely did the standard deviation of the ozone sampled change by more than 5 DU during a morning or afternoon when Langleys plots are sampled. This small change is typical for this low latitude.

Moved (insertion) [2]

Deleted: 2



150
 151 **Figure 2.** Plot of ozone measured by a Dobson unit at Mauna Loa Observatory retrieved using the Dobson AC
 152 pair versus the Dobson AD pair. Solid diagonal line is 1:1 line and dashed line is linear least-squares fit. The
 153 mean difference and standard deviation of the samples are given on the plot.
 154
 155

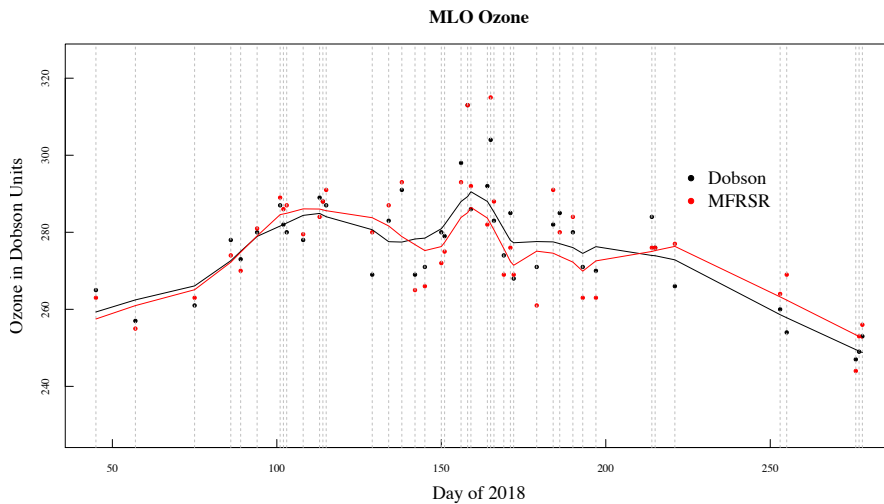
Deleted: 2

156 wavelength pairs. The mean difference in retrieved ozone for the 90 points compared in the plot
 157 is less than 0.5 DU and the standard deviation among the 90 samples is close to 2.5 DU.
 158 Therefore, using the AC pair of the UV-MFRSR for ozone retrievals and comparing to AD-pair
 159 Dobson ozone should be acceptable.
 160

161 Figure 3 is a plot of the ozone time series retrieved from the Dobson AD pair and the UV-
 162 MFRSR AC pair for the 2018 data that were matched by day of year. In the case of the Dobson,

Deleted: 3

165 one measurement is chosen from the three daily measurements made at 1000, 1200 and 1400



166
167 **Figure 3.** Time series plot of Mauna Loa Observatory for 43 days of retrieved ozone for 2018 using the
168 Dobson spectrophotometer (black dots) and the UV-MFRSR (red dots). The lines are lowest fits using 0.25 of
169 the points for the lowest fit at each point. The Dobson uses one of three measured points for the daily value,
170 and the UV-MFRSR uses the median of all 20-second, clear-sun data for air masses less than three.

Deleted: 3

171
172
173 local standard time. Only direct sun measurements made with the Dobson are used for this
174 comparison. For the UV-MFRSR data, which is sampled every 20 seconds, a median value of all
175 points, which are made at less than three air masses and that pass cloud-screening (Michalsky et
176 al., 2010), is used. Since measurements from the two instruments are made differently and no
177 attempt to make them coincident, except for occurring on the same day, there is no expectation
178 of perfect agreement given any diurnal variability. The average difference over the 43-day
179 sample is about 0.10 Dobson units. The lowest fits to the two data sets track each other rather
180 closely matching dips and peaks throughout the measurement period.

Deleted: (Michalsky et al., 2010)

181 182 Sources of Ozone Uncertainty

183
184
185 Uncertainties in using a UV-MFRSR for ozone retrievals were discussed thoroughly by Gao et
186 al. (2001). In this paper only data taken at less than three air masses (about 71° solar-zenith
187 angle) were used because (1) air mass determination is less certain at higher solar-zenith angles
188 and the cosine response correction for the UV-MFRSR is larger and more difficult to pinpoint
189 and, therefore, more uncertain. The extraterrestrial responses for the four filters used to retrieve
190 ozone were averages for the 242-day period in 2018 as stated earlier. The uncertainties in
191 extraterrestrial responses were between 0.2% and 0.3%. The ozone absorption coefficients were
192 those measured by Bass and Paur (1985) adjusted for mid-latitude seasonal variations. The
193 effective ozone absorption coefficients were determined by convolving each of the four filter

Deleted: ozone

Deleted: were determined by convolving

Formatted: Strikethrough

198 profiles ~~with the wavelength dependent~~ Bass and Paur (1985) ~~ozone absorption coefficients~~.
199 ~~Similarly, effective Rayleigh scattering optical depths were determined in the same manner. The~~
200 ~~effective~~ Rayleigh optical depths were pressure corrected using on-site measurements of
201 atmospheric pressure.

Deleted: with the wavelength dependent

Deleted: ozone absorption coefficients

Moved down [3]: Similarly, effective Rayleigh scattering optical depths were determined in the same manner.

Moved (insertion) [3]

Deleted: effective

203 Always a major concern when working in the ultraviolet is light from outside the band passes
204 contributing to the measured signal. Si-C (silicon carbide) is the detector for the 300 nm and 305
205 nm filters. GaP (gallium phosphide) is used as the detector in the five longest wavelength filters.
206 To measure the extent of the possible long-wavelength leakage, we used a Schott glass OG530
207 placed over the entrance optic being careful to block light paths from the edges that might reach
208 the entrance diffuser optic. The transmission below 460 nm is 0.00001, therefore no light should
209 reach the detectors with the OG530 completely covering the entrance optic. If higher orders of
210 light from the interference filters would reach the detectors, they would begin to be a problem
211 around 600 nm for the 300-nm filter and at longer wavelengths for the other six filters. The
212 nighttime dark readings and 530 Schott blocking filter readings on a clear, sunny day were
213 compared. These readings agreed within the detection limit for the UV-MFRSR.

216 Aerosol Optical Depth Retrievals

217 After subtracting the large ozone and Rayleigh optical depth contributions to the total optical
218 depth, a residual remains that is assumed to be aerosol extinction. ~~Historically, At~~ Mauna Loa
219 Observatory the aerosol optical depths (AODs) are, in most cases, very small in the visible
220 except in the aftermath of volcanic eruptions (Dutton et al., 1994). The current paper examines
221 AODs in the ultraviolet near 305.6, 311.4, 317.5, 325.1, 332.4, and 367.8 nm where
222 measurements of AOD are infrequently made, ~~especially below 340 nm~~. These wavelengths are
223 shorter than those measured by most sunphotometers ~~except for the 368-nm wavelength, with~~
224 ~~340 nm the shortest wavelength measured by AERONET (Holben et al., 2001), for example,~~
225 ~~Recently, however, López-Solano et al. (2018) used Brewer spectrophotometers to derive AODs~~
226 ~~at five wavelengths between 306.3 and 320.1 nm. They compared AODs measured in this~~
227 ~~wavelength range by different co-located Brewers and the UVPFR (Carlund et al., 2017). In~~
228 ~~general, there was excellent agreement between the Brewers and good, but less satisfactory,~~
229 ~~agreement between Brewers and the UVPFR, however, there was no discussion of the~~
230 ~~wavelength dependence of the Brewer and UVPFR AODs at these low wavelengths, which we~~
231 ~~consider next.~~

Deleted: A

Formatted: Strikethrough

Deleted: , especially below 340 nm

Moved down [4]: with 340 nm the shortest wavelength measured by AERONET (Holben et al., 2001), for example. Recently, however, López-Solano et al. (2018) used Brewer spectrophotometers to derive AODs at five wavelengths between 306.3 and 320.1 nm. They compared AODs measured in this wavelength range by different co-located Brewers and the UVPFR (Carlund et al., 2017). In general, there was excellent agreement between the Brewers and good, but less satisfactory, agreement between Brewers and the UVPFR, however, there was no discussion of the wavelength dependence of the Brewer and UVPFR AODs at these low wavelengths, which we consider next.

Moved (insertion) [4]

Formatted: Strikethrough

Deleted: 4

Moved down [5]: The red point in Fig. 4 is the average of co-located AERONET data at 340.8 nm (Holben et al., 2001) taken during the same time as the average of the UV-MFRSR data plotted here. This plot indicates consistency between the AERONET and UV-MFRSR data beyond 332 nm.

Moved (insertion) [5]

Formatted: Strikethrough

Deleted: exhaustive analysis of uncertainties in the UVPFR

Deleted: this

Deleted: at the shortest

Deleted: ultraviolet wavelengths close to those of our UV-MFRSR could

235 Figure 4 is typical of the AOD versus wavelength plots from the 43 days of measurements
236 plotted in Fig. 3. *Typical visible* wavelength dependent behavior indicates a negative slope on
237 this type of plot, however, the slope is positive from 305 to 332 nm and then becomes negative
238 after that, with the 368-nm wavelength AOD smaller than the 332-nm wavelength. The red point
239 in Fig. 4 is the average of co-located AERONET data at 340.8 nm (Holben et al., 2001) taken
240 during the same time as the average of the UV-MFRSR data plotted here. This plot indicates
241 consistency between the AERONET and UV-MFRSR data beyond 332 nm. A careful search for
242 systematic errors in a, exhaustive analysis of uncertainties in the UVPFR paper by Carlund et al.
243 (2017) that examines another narrowband filter instrument at the shortest ultraviolet wavelengths

275 close to those of our UV-MFRSR could not explain the similar wavelength dependence (see the
 276 right-hand-side of their Fig. 6) that they measured for low aerosol optical depth days in the
 277 autumn at Davos, Switzerland. Their Figure 7 supports the argument that the Brewer
 278 spectrophotometer measurements at similar wavelengths should return a similar wavelength
 279 dependence. However, data from Davos in the spring did not show the downturn in AOD at the
 280 shortest wavelengths that the autumn data indicated. In summary, Carlund et al. (2017) suggests
 281 that the size of the uncertainties cannot completely rule out the possibility of a more typical
 282 wavelength dependence with AOD increases with decreasing wavelength.

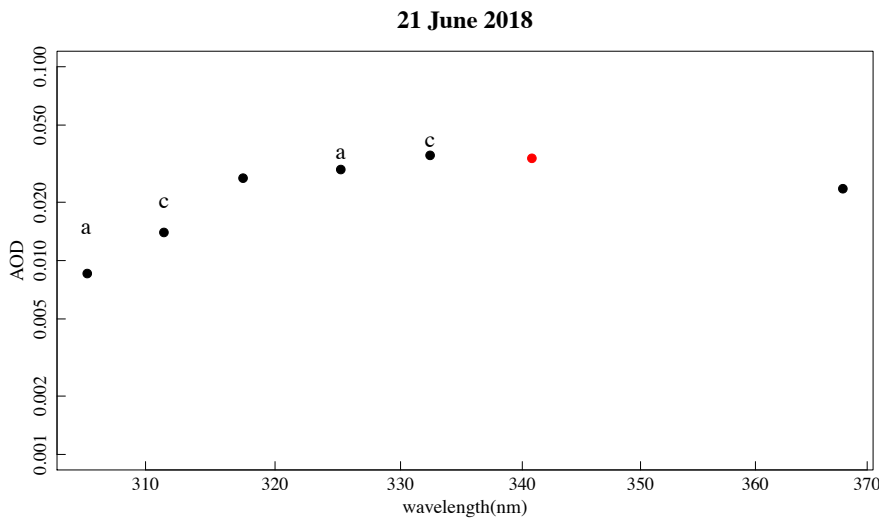
283
 284 We also looked at nitrogen dioxide (NO₂) as a possible contaminant that if not removed could
 285 explain this wavelength behavior, however, the typical amount of NO₂ in the column above
 286 Mauna Loa would necessitate a correction of less than 0.001 optical depths at 332 nm, less at the
 287 shorter wavelengths, and slightly more at 368 nm. When only considering the 332 nm and 368
 288 aerosol optical depths the plot indicates the typical visible wavelength dependence. Although
 289 Fig. 4 is the only plot of AOD shown, all of the 43 days had similar behavior.

Deleted: in the autumn

Moved down [6]: Their Figure 7 supports the argument that the Brewer spectrophotometer measurements at similar wavelengths should return a similar wavelength dependence. However, data from Davos in the spring did not show the downturn in AOD at the shortest wavelengths that the autumn data indicated. In summary, Carlund et al. (2017) suggests that the size of the uncertainties cannot completely rule out the possibility of a more typical wavelength dependence with AOD increases with decreasing wavelength.

Moved (insertion) [6]

Deleted: 4



293
 294 **Figure 4.** This plot indicates the AOD versus wavelength for the UV-MFRSR filter set at Mauna Loa
 295 Observatory. Instead of a negative slope, this figure, which is typical of the 43 days in this study, indicates a
 296 positive slope with a negative slope indicated only by the two longest wavelengths. The 'a' and 'c' labels are
 297 included to indicate the wavelength pairs used for the ozone retrievals. The red point is the average of the
 298 AERONET points at 340.8 nm that overlap with the UV-MFRSR averaging period.

Deleted: 4

Moved down [7]: The red point is the average of the AERONET points at 340.8 nm that overlap with the UV-MFRSR averaging period.

Moved (insertion) [7]

301 Discussion

318
319 This paper focuses on data from the Manua Loa Observatory only. It corroborates results
320 reported by Gao et al. (2001) regarding the UV-MFRSR's ability to retrieve ozone column that is
321 in agreement with the Dobson instrument at Mauna Loa Observatory. Figure 3 demonstrates this
322 agreement even though there was no attempt to synchronize ozone observations other than to
323 have them occur on the same day.

324
325 Aerosol optical depths were measured in this very clean environment with expected low values,
326 but an unexpected wavelength dependence. This wavelength dependence is similar to that
327 obtained with an independent, sun-pointed narrowband filter instrument developed and operated
328 at the World Radiation Center (WRC) in Davos, Switzerland. Our and the WRC's attempts to
329 explain this wavelength dependence have yet to yield an understanding of the physics at work
330 here. Systematic biases may be responsible; a better understanding of the very large optical
331 depths associated with ozone absorption and Rayleigh scattering at these wavelengths that have
332 to be subtracted to obtain the small AOD at these wavelengths may require more investigation.
333 On the other hand, further study of environments with somewhat larger aerosol optical depths
334 may indicate that this is, perhaps, associated with aerosol size distributions in some conditions.

335 336 Appendix

337
338 After the paper was accepted as a preprint in Atmospheric Measurement Techniques we were
339 contacted by Alexander Smirnov of the AERONET team (aeronet.gsfc.nasa.gov). He made us
340 aware of early Russian papers that measured AODs near the same short UV wavelengths that are
341 plotted in Figure 4. These are discussed in a book by Rozenberg (1966) that was originally
342 published in Russian in 1963, and translated to English for the 1966 publication in the reference
343 list. Figure 97 in the Rozenberg (1996) book is a reproduction of the figure from the paper by
344 Rodionov et al. (1942) that clearly shows AOD decreasing shortward of 380 nm (dubbed by
345 these authors "anomalous transparency"). The observations were made at a high (3 km)
346 mountain site explaining the low AOD values. These authors suggested that a specific aerosol
347 size distribution might explain their wavelength dependence. Rodionov et al.'s (1942)
348 measurements and suggested explanation of them were criticized, but a paper by Sakerin et al.
349 (2000) suggesting that this effect and other unusual spectral dependencies of the AOD could be
350 explained theoretically using specific combinations of nucleation, accumulation, and coarse
351 aerosol modes.

352
353 *Author contributions:* JM drafted the paper and produced the figures. GM produced the data for
354 Fig. 2 and provided details about the Dobson ozone retrievals using the AD and AC pairs.

355
356 *Competing interests.* The contact author has declared that none of the authors has any competing
357 interests.

358
359 *Acknowledgments.* This paper benefited from Dobson ozone retrieval discussions with Peter
360 Effertz and Irina Petropavlovskikh. Kathy Lantz provided the UV-MFRSR data from Mauna Loa
361 Observatory and performed the out-of-band rejection studies. Gary Morris and Kathy Lantz
362 provided a careful reading of the draft paper. Thomas Carlund provided useful insight on WRC's
363 efforts at ultraviolet AOD retrievals using the World Radiation Center (WRC) UV-PFR while he

Moved down [8]: Appendix

After the paper was accepted as a preprint in Atmospheric Measurement Techniques we were contacted by Alexander Smirnov of the AERONET team (aeronet.gsfc.nasa.gov). He made us aware of early Russian papers that measured AODs near the same short UV wavelengths that are plotted in Figure 4. These are discussed in a book by Rozenberg (1966) that was originally published in Russian in 1963, and translated to English for the 1966 publication in the reference list. Figure 97 in the Rozenberg (1996) book is a reproduction of the figure from the paper by Rodionov et al. (1942) that clearly shows AOD decreasing shortward of 380 nm (dubbed by these authors "anomalous transparency"). The observations were made at a high (3 km) mountain site explaining the low AOD values. These authors suggested that a specific aerosol size distribution might explain their wavelength dependence. Rodionov et al.'s (1942) measurements and suggested explanation of them were criticized, but a paper by Sakerin et al. (2000) suggesting that this effect and other unusual spectral dependencies of the AOD could be explained theoretically using specific combinations of nucleation, accumulation, and coarse aerosol modes.

Moved (insertion) [8]

Field Code Changed

Deleted: Gary Morris and Kathy Lantz

391 was on sabbatical at the WRC in Davos, Switzerland. Alexander Smirnov was very helpful in
392 pointing out and discussing the earlier papers on Russian measurements and possible
393 explanations for the low UV short wavelength AODs.

394
395

396 *Financial support.* The publication costs for this paper were covered by the Global Monitoring
397 Laboratory of the National Oceanic and Atmospheric Administration.

398
399

400 References

401

402 Bass, A. M. and Paur, R. J. 1985: The ultraviolet cross sections of ozone: I. The measurements.
403 In Atmospheric Ozone - Proceedings of the Quadrennial Ozone Symposium 1984, (Editors: C.S.
404 Zerefos and A. Ghazi), pp. 606-610, Springer, Dordrecht. [https://doi.org/10.1007/978-94-009-](https://doi.org/10.1007/978-94-009-5313-0_120)
405 [5313-0_120](https://doi.org/10.1007/978-94-009-5313-0_120), 1985.

406

407 Bohdaine, B. A., Wood, N. B., Dutton, E. G., Slusser, J. R.: On Rayleigh optical depth
408 calculations. J. Atmos. Ocean. Tech., 16, 1854-1861, [https://doi.org/10.1175/1520-](https://doi.org/10.1175/1520-0426(1999)016<1854:ORODC>2.0.CO;2)
409 [0426\(1999\)016<1854:ORODC>2.0.CO;2](https://doi.org/10.1175/1520-0426(1999)016<1854:ORODC>2.0.CO;2), 1999.

410

411 Carlund, T., Kouremeti, N., Kazadzis, S., and Gröbner, J.: Optical depth determination in the UV
412 using a four-channel precision filter radiometer. Atmos. Meas. Tech., 10, 905-923,
413 [doi:10.5194/amt-10-905-2017](https://doi.org/10.5194/amt-10-905-2017), 2017.

414

415 Dutton, E. G., Reddy, P., Ryan, S., and DeLuisi, J. J.: Features and effects of aerosol optical
416 depth observed at Mauna Loa, Hawaii: 1982-1992. J. Geophys. Res., 99, 8295-8306,
417 doi.org/10.1029/93JD03520, 1994.

418

419 Gao, W., Slusser, J., Gibson, J., Scott, G., Bigelow, D., Kerr, J. and McArthur, B.: Direct-Sun
420 column ozone retrieval by the ultraviolet multifilter rotating shadow-band radiometer and
421 comparisons with Brewer and Dobson spectrophotometers. Appl. Optics, 40, 3149-3155, [doi:](https://doi.org/10.1364/AO.40.003149)
422 [10.1364/AO.40.003149](https://doi.org/10.1364/AO.40.003149), 2001.

423

424 Holben, B. N., Tanre, D., Smirnov, A., Eck, T. F., Slutsker, I., Abuhassan, N., Newcomb, W. W.,
425 Schafer, J., Chatenet, B., Lavenue, F., Kaufman, Y. J., Vande Castle, J., Setzer, A., Markham,
426 B., Clark, D., Frouin, R., Halthore, R., Karnieli, A., O'Neill, N. T., Pietras, C., Pinker, R. T.,
427 Voss, K., and Zibordi, G.: An emerging ground-based aerosol climatology: Aerosol optical depth
428 from AERONET, J. Geophys. Res., 106, 12067-12097, <https://doi.org/10.1029/2001JD900014>,
429 2001.

430

431 Komhyr, W. D. Operations Handbook—Ozone Observations with a Dobson Spectrophotometer,
432 rev., Evans, R. D., AW No. 183, WMO/TD -No. 1469, 2008.

433

434 López-Solano, J., Redondas, A., Carlund, T., Rodríguez-Franco, J. J., Diémoz, H., León-Luis, S.,
435 F., Hernández-Cruz, B., Guirado-Fuentes, C., Kouremeti, N., Gröbner, J., Kazadzis, S., Carreño,
436 V., Berjón, A., Santana-Díaz, D., Rodríguez-Valido, M., De Bock, V., Moreta, J. R., Rimmer, J.,

Moved down [9]: Alexander Smirnov was very helpful in pointing out and discussing the earlier papers on Russian measurements and possible explanations for the low UV short wavelength AODs.

Moved (insertion) [9]

Moved down [10]: Bohdaine, B. A., Wood, N. B., Dutton, E. G., Slusser, J. R.: On Rayleigh optical depth calculations. J. Atmos. Ocean. Tech., 16, 1854-1861, [https://doi.org/10.1175/1520-0426\(1999\)016<1854:ORODC>2.0.CO;2](https://doi.org/10.1175/1520-0426(1999)016<1854:ORODC>2.0.CO;2), 1999.¶

Moved (insertion) [10]

Field Code Changed

Moved down [11]: Holben, B. N., Tanre, D., Smirnov, A., Eck, T. F., Slutsker, I., Abuhassan, N., Newcomb, W. W., Schafer, J., Chatenet, B., Lavenue, F., Kaufman, Y. J., Vande Castle, J., Setzer, A., Markham, B., Clark, D., Frouin, R., Halthore, R., Karnieli, A., O'Neill, N. T., Pietras, C., Pinker, R. T., Voss, K., and Zibordi, G.: An emerging ground-based aerosol climatology: Aerosol optical depth from AERONET, J. Geophys. Res., 106, 12067-12097, <https://doi.org/10.1029/2001JD900014>, 2001.¶

Komhyr, W. D. Operations Handbook—Ozone Observations with a Dobson Spectrophotometer, rev., Evans, R. D., AW No. 183, WMO/TD -No. 1469, 2008.¶

López-Solano, J., Redondas, A., Carlund, T., Rodríguez-Franco, J. J., Diémoz, H., León-Luis, S. F., Hernández-Cruz, B., Guirado-Fuentes, C., Kouremeti, N., Gröbner, J., Kazadzis, S., Carreño, V., Berjón, A., Santana-Díaz, D., Rodríguez-Valido, M., De Bock, V., Moreta, J. R., Rimmer, J., Smedley, A. R. D., Boukkelia, L., Jepsen, N., Eriksen, P., Bais, A. F., Shirov, V., Vilaplana, J. M., Wilson, K. M., and Karppinen, T.: Aerosol optical depth in the European Brewer Network, Atmos. Chem. Phys., 18, 3885-3902, <https://doi.org/10.5194/acp-18-3885-2018>, 2018.¶

Michalsky, J., Denn, F., Flynn, C., Hodges, G., Kiedron, P., Koontz, A., Schlemmer, J., and Schwartz, S. E.: Climatology of aerosol optical depth in north-central Oklahoma: 1992-2008, J. Geophys. Res., D07203, <https://doi.org/10.1029/2009JD012197>, 2010.¶

Michalsky, J., Schlemmer, J., Berkheiser III, W., Berndt, J., Harrison, L., Laulainen, N., Larson, N., and Barnard, J.: Multi-year measurements of aerosol optical depth in the Atmospheric Radiation Measurement and Quantitative Links programs, J. Geophys. Res., 106, 12099-12107, <https://doi.org/10.1029/2001JD900096>, 2001.¶

Moved (insertion) [11]

Field Code Changed

490 [Smedley, A. R. D., Boulkelia, L., Jepsen, N., Eriksen, P., Bais, A. F., Shirov, V., Vilaplana, J.](#)
491 [M., Wilson, K. M., and Karppinen, T.: Aerosol optical depth in the European Brewer Network,](#)
492 [Atmos. Chem. Phys., 18, 3885–3902, <https://doi.org/10.5194/acp-18-3885-2018>, 2018.](#)
493
494 [Michalsky, J., Denn, F., Flynn, C., Hodges, G., Kiedron, P. Koontz, A., Schlemmer, J., and](#)
495 [Schwartz, S. E.: Climatology of aerosol optical depth in north-central Oklahoma: 1992:2008, J.](#)
496 [Geophys. Res., D07203, <https://doi.org/10.1029/2009JD012197>, 2010.](#)
497
498 [Michalsky, J., Schlemmer, J., Berkheiser III, W., Berndt, J., Harrison, L., Laulainen, N., Larson,](#)
499 [N., and Barnard, J.: Multi-year measurements of aerosol optical depth in the Atmospheric](#)
500 [Radiation Measurement and Quantitative Links programs, J. Geophys. Res., 106, 12099-12107,](#)
501 [https://doi.org/10.1029/2001JD900096, 2001.](#)
502
503 [Rozenberg, G.V.: Twilight: A Study in Atmospheric Optics, Plenum Press, New York, 358 pp.,](#)
504 [ISBN 0608129313, 9780608129310, 1996. \(Originally published in Moscow by State Press for](#)
505 [Physico Mathematical Literature 1963.\)](#)
506
507 [Rodionov, S. F., Pavlova, E. N., Rdultovshaya, E. V. and Reinov, N. T.: Izv. Nauk SSSR, Ser.](#)
508 [Geogr. Geofiz., 6, No. 4, 135 \(1942\).](#)
509
510 [Sakerin, S. M., Rakhimov, R. F., Makienko, E. V., and Kabanov, D. M.: Interpretation of the](#)
511 [anomalous spectral dependence of the aerosol optical depth in the atmosphere. Part I. Formal](#)
512 [analysis of situation, Atmos. Oceanic Opt, 13, No. 9, 754-758, 2000.](#)
513
514 Staehelin, J., Kerr, J., Evans, R. and Vanicek, K., Comparison of total ozone measurements of
515 Dobson and Brewer spectrophotometers and recommended transfer functions, WMO/GAW 149
516 (WMO TD 1147), 39 pp., 2003.

Field Code Changed

Field Code Changed

Field Code Changed

Moved down [12]: Rozenberg, G.V.: Twilight: A Study in Atmospheric Optics, Plenum Press, New York, 358 pp., ISBN 0608129313, 9780608129310, 1996. (Originally published in Moscow by State Press for Physico Mathematical Literature 1963.)

⚡
Rodionov, S. F., Pavlova, E. N., Rdultovshaya, E. V. and Reinov, N. T.: Izv. Nauk SSSR, Ser. Geogr. Geofiz., 6, No. 4, 135 (1942).⚡

⚡
Sakerin, S. M., Rakhimov, R. F., Makienko, E. V., and Kabanov, D. M.: Interpretation of the anomalous spectral dependence of the aerosol optical depth in the atmosphere. Part I. Formal analysis of situation, Atmos. Oceanic Opt, 13, No. 9, 754-758, 2000.⚡

Moved (insertion) [12]